

# Smart fabrics that think, sense, and act.

**A scalable, modular approach to in-place printed strain sensors**

Bachelor thesis by Philipp Macher (Student ID: 2256373)

Date of submission: September 3, 2025

1. Review: Gutachter 1

2. Review: Gutachter 2

Darmstadt



TECHNISCHE  
UNIVERSITÄT  
DARMSTADT

Computer Science  
Department

Resilient Cyberphysical  
Systems

# Contents

---

<b>1. Introduction</b>	<b>4</b>
<b>2. Related Work</b>	<b>5</b>
<b>3. Concept</b>	<b>9</b>
3.0.1. Layout . . . . .	10
<b>4. Design</b>	<b>11</b>
4.1. Sensor Design . . . . .	11
4.1.1. Model . . . . .	11
4.1.2. Sensor layout . . . . .	13
4.1.3. Integrating the Sensor . . . . .	14
4.2. Compute Node Design . . . . .	16
4.2.1. Choosing Hardware . . . . .	16
4.3. A Modular Network . . . . .	18
4.3.1. Wireless Protocols . . . . .	19
4.3.2. Wirebound Protocol Candidates . . . . .	19
4.3.3. CAN Bus . . . . .	20
<b>5. Implementation</b>	<b>24</b>
5.1. First Physical Compute Node . . . . .	24
5.1.1. PCB Design . . . . .	27
5.2. Prototyping a sensor . . . . .	28
5.2.1. Voltera NOVA . . . . .	28
5.2.2. Sensor V1 . . . . .	30
5.2.3. Sensor V2 . . . . .	31
5.2.4. Sensor V3 . . . . .	32
5.2.5. Manufacturing pitfalls . . . . .	34

---

---

<b>6. Results and Analysis</b>	<b>35</b>
6.1. Sensor prototype V2 . . . . .	35
<b>7. Conclusion</b>	<b>36</b>
<b>8. Discussion</b>	<b>37</b>
<b>A. Formulas and derivations</b>	<b>43</b>
A.1. Trace height in relation to bending angle . . . . .	43
<b>B. Example values</b>	<b>44</b>
B.1. Example sensor setup . . . . .	44
<b>C. Hardware Implementation</b>	<b>45</b>
<b>D. Risk Assessment NOVA</b>	<b>48</b>
<b>E. SC1502</b>	<b>51</b>
E.1. Data Sheet . . . . .	51
E.2. Safety Data Sheet . . . . .	54

---

# 1. Introduction

---

Smart everything is on the rise. Increasingly, approaches to smart fabrics are being explored, offering new possibilities for materials that provide more functionality than their predecessors, such as actuation on a miniaturized scale, adjustable properties, or new sensing capabilities. Many approaches focus on deploying new sensors embedded directly into the fabric to enable measurements over the entire area of the fabric[15]. Distributed sensing is vital in the medical field, sports, robotics, and even our daily lives, for example, to support sign language translation[31]. Pulse, muscular activity, joint articulation, and pressure/touch sensing are just a few of the sensed properties that have been explored. We aim to provide an easily reproducible, adaptable, scalable, and modular approach to the distributed sensing of a fabric's articulation, specifically the degree to which it is stretched and bent in certain areas. If the articulation of a fabric is known, that offers many use cases: Very adaptable measuring of joint articulation of a broad range of robotic joints, measuring deformation of whole planes as in crash tests or medical chairs[26], connecting multiple moving robots and enabling them to know their relation to each other by connecting them with such a fabric.

This work will examine the existing literature and propose a novel approach to developing modular, scalable smart fabrics. This new approach focuses on the reading of sensor outputs throughout the fabric and passing them to a reader in a way that is more scalable than all currently available alternatives. To demonstrate the functionality of this approach, a small smart fabric is produced. In this context, a basic strain sensor is designed to measure its strain and bending angle. Additionally, a compute node prototype is developed and built to measure the fabric and communicate the results.

## 2. Related Work

---

### Smart fabrics as a broad field

Hassabo et al.[8] provide a comprehensive overview of the extensive field of research in smart fabrics. Smart fabrics can be an umbrella term for various approaches to creating smart functionality on any type of fabric. The "Fabric" in smart fabrics does not necessarily need to be a textile, but can be any composite material consisting of smart components. Additionally, "Smart" lacks a concrete definition. It may involve computation, sensing, actuation, modification of the fabric's responses or behavior, or passively provided features beyond the norm.

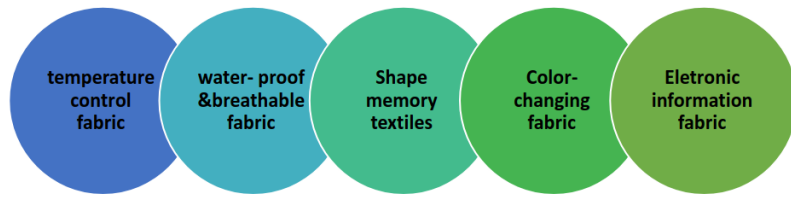


Figure 2.1.: Applications of SMART fabrics, from Hassabo et al[7]

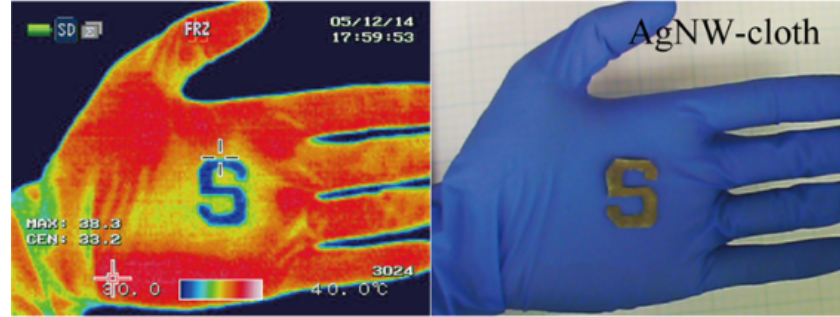
Examples of these different smart features might include materials with varying stiffness, as demonstrated by Yuen et al.[32], or shape memory materials, as developed by Huan et al.[12]. Passive features might be better temperature regulation[13, 10] or water evaporation[5, 14], for example.

### Sensing smart fabrics

Many approaches to smart fabrics, classified as passive smart fabrics, focus on sensing the environment of the fabric in a new way and making these measurements accessible to



(a) Fabric with variable stiffness by Yuen et al[32] (b) Shape memory fabric by Yuen et al[12] (c) Fabric with improved water evaporation by Fan et al[5]



(d) Fabric with better heat dissipation than skin by Hsu et al[10]

Figure 2.2.: Four smart fabric domain examples: a) varying stiffness; b) shape memory; c) temperature control; d) water evaporation

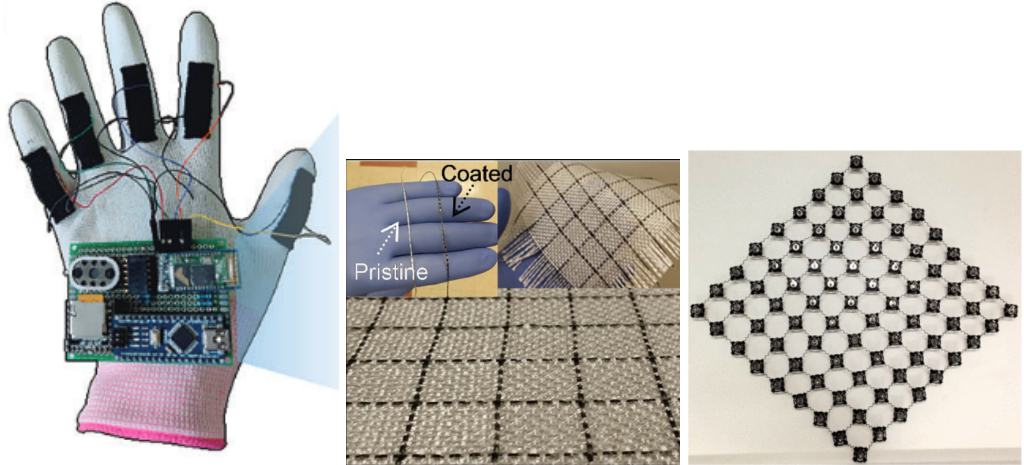
the user or further components. For this, various new technologies are being explored to enable smart fabrics to measure the desired properties. In this field, a significant concern are strain sensors, as they are crucial for measuring the activity of the human body[9]. While flexible strain sensors are already commercially available, stretchable strain sensors represent a new level of wearability, as most fabrics and wearables are stretchable themselves. Trung et al.[29] built a very easily attachable, intrinsically stretchable, and transparent strain sensor from multiple layers of different polymers to measure strain and temperature. Souri et al.[25] provide an overview of additional wearable strain sensing technologies, including some utilizing carbon nanotubes, nanofibers, conductive polymers, and strain sensors in the form of optical fibers, among others.

This work focuses on the development of a highly scalable, modular robotic fabric incorporating flexible strain sensors. While most papers in this domain focus on creating a single sensor to be integrated into its area of operation, this work presents an adaptable and easily reproducible strain sensor, along with an approach to a scalable network comprising multiple sensors. Scalable sensor networks are crucial for smart fabric applications, as sensors in smart fabrics, in theory, often offer a high sensor density that needs to be supported by a network to read and process all these measurements. There is literature about easily scalable network topologies to be used for such a network to optimize area coverage while using as few nodes as possible and keeping network integrity at a high level[3, 28].

## Similar work

Wu et al.[31] construct a stretchable strain sensor from a laser-cut and partially electroplated carbon fiber reinforced polymer. With these sensors, they build a smart fabric consisting of 5 sensors and a compute node in the form of a glove, shown in Fig.2.3a. The compute node reads all the strain sensors, interprets the values of the finger sensors, translates them into words, emits the translation through text-to-speech (TTS) synthesis, and transmits the translation wirelessly over Bluetooth to another computer for human confirmation. Their work involves the reading of multiple sensors by a compute node located on the fabric, transmitting results to a computer for further processing. However, it lacks intra-fabric networking and scalability, though scalability beyond 2 gloves would most likely not be necessary.

Luo et al.[15] developed an easily scalable and highly adaptable sensor array using fiber-glass roving coated with multi-walled carbon nanotubes, which was further processed. The resulting fiber can be woven into fabrics and acts as a single sensor. This makes



(a) A glove equipped with five strain sensors for sign language translation, by Wu et al[31]

(b) CNT based woven strain sensor to sense strain in a 2D grid, by Luo et al[15]

(c) A smart fabric consisting of small robots, connected by springs, by Obilikpa et al[19]

it very easy to weave multiple fibers vertically and horizontally into a fabric with easily adaptable sensing precision by adjusting the relation of sensing and regular fibers. The end result is a fabric that can sense strain in a 2D grid. Luo et al. focus on the sensor array aspect in this work, but do not present a scalable approach to reading these sensors in a way that is as scalable as the fibers themselves are.

Obilikpa et al.[19] proposed a robotic fabric consisting of multiple battery-powered robots, connected by rigid or flexible links. They estimate their position in relation to their neighbors by broadcasting infrared (IR) messages. The robots can move individually, but their movement is inaccurate. Utilizing Motion Control Algorithms (MCA)[20], the movement error for each robot can be overcome in the fabric, and the fabric can move coherently. This concept lacks the information about the articulation of the complete fabric in any single location. This is mostly overcome by the chosen MCAs. The communication over IR is dependent on the surface the robots are walking on and can be manipulated by a change in the reflectiveness of the surface the fabric is moving over.

## 3. Concept

---

Most work in this area concentrates on creating novel sensors, and nearly all of these newly developed sensors are not trivial to reproduce. Additionally, few works actually utilize these technologies to build a robotic fabric. This work concentrates on these aspects. The focus lies on creating stretchable robotic fabric and proposing a concept that is modular and easily scalable, implementing the sensors, compute nodes, and their connection. As the sensors are a central part of such a fabric, we'll need to fabricate strain sensors. As the strain sensors introduced in the related work are complex to build and need fabrication techniques our lab does not offer, we'll develop our own, easier-to-reproduce sensors.

The smart fabric should ultimately be able to perform proprioception, allowing it to sense how it is articulated. This means that the fabric should be able to measure where and how much it is strained, at least. If possible, it should be able to differentiate between being bent and being stretched, as no other work measures both stretching and bending a fabric separately. The fabric should be modular, so it shall be trivial to add more nodes and sensors to the fabric. It shall also be scalable and support hundreds of nodes in theory. Also, the resulting data should be collectible from a single connection point. Adaptability, although not a primary goal, is another concern, as fabrics should be easily adaptable to meet specific needs in terms of form and sensing accuracy.

Summarized, this leads to the following requirements:

- The fabric shall contain strain, or bend- and stretch-sensors for Proprioception
- These sensors shall be easy to build and reproduce
- The concept shall be modular, so easily extendable
- The concept shall be scalable and support a high number of nodes
- Data shall be retrievable from a single connection

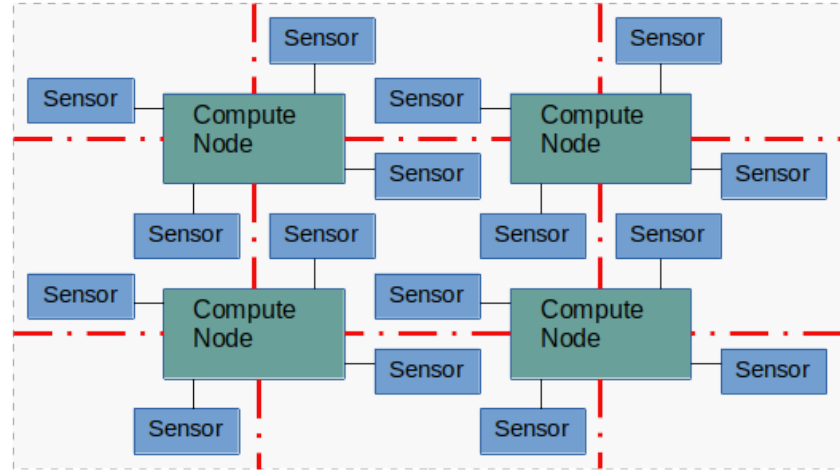


Figure 3.1.: Concept sketch

The concept proposed here is a fabric consisting of small sensors, distributed over a stretchable substrate, a sketch is shown in Fig. 3.1. The sensors are being read out by compute nodes sitting in between them, with a single compute node reading out multiple sensors. The compute nodes themselves are interconnected by a communication and power bus. The chosen communication protocol must allow for the easy addition and removal of sensors, while also being scalable. All readings must be processed and distributed in a manner that allows querying them from a single compute node.

### 3.0.1. Layout

While the concept covers how Nodes and sensors are connected, this section presents an example layout consisting of four compute nodes and eight sensors

TODO Bild bauen.

## 4. Design

### 4.1. Sensor Design

#### 4.1.1. Model

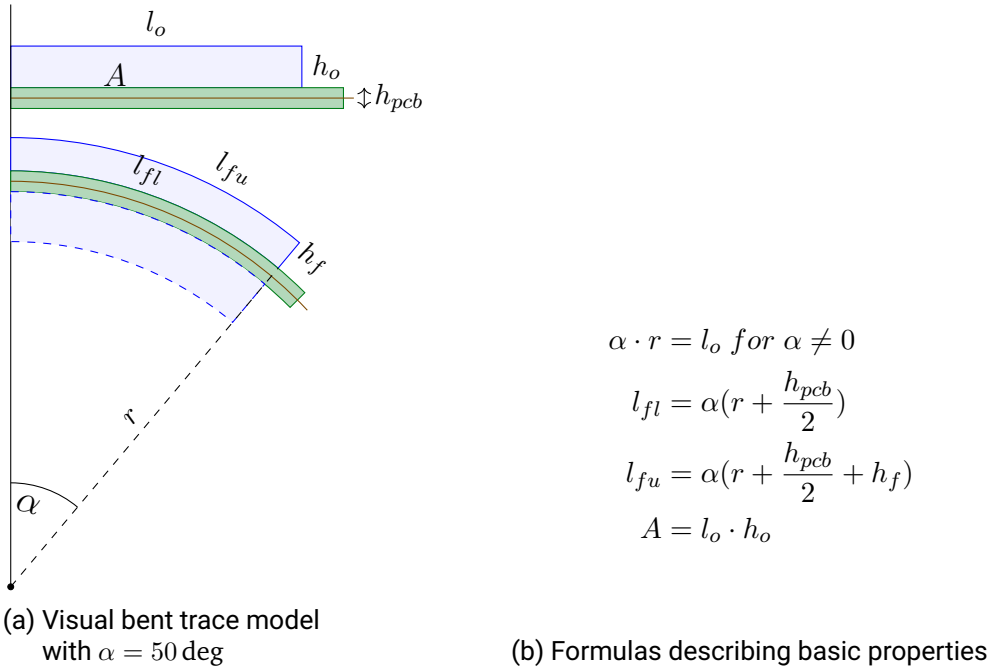


Figure 4.1.: Model of a bent conductor trace on a flexible PCB

One focus of this work is to create simple, adaptable strain sensors for use in the smart fabric network. Before building these sensors, a model is required to perform calculations

and determine the feasibility of such a sensor. Similar to common strain gauges, as in [2], we measure the resistance of a conductor, which changes depending on the degree of deformation.

Imagining a trace of conductive ink on a flex substrate with the substrate being bent, the assumption is made that the trace width does not change significantly. But the total volume of the trace still stays the same (so, the density of the ink does not change under bending or stretching).

When the substrate is bent, the trace lying on one side (where the substrate is bent away from) becomes longer, while a trace on the other side becomes shorter. The constant width and area of the traces lead to an induced change in height for both traces. Fig. 4.1a illustrates that with a cross-sectional view of a trace. Fig. 4.1b lists some basic equations describing the model.

To approximate the expected change in resistance,  $h_f$  has to be calculated. Solving the formulas in 4.1b for  $h_f$ , as shown in ?? leads to the two resulting equations 4.1.  $h_{f+}$  is the only plausible candidate and is used for  $h_f$ .

$$h_{f+/-} = -\frac{l_o}{\alpha} - \frac{h_{pcb}}{2} \pm \sqrt{\frac{h_{pcb}^2}{4} + \frac{l_o h_{pcb}}{\alpha} + \frac{l_o^2}{\alpha^2} + \frac{2l_o h_o}{\alpha}} \quad (4.1)$$

$$h_{f+/-} = \frac{l_o}{\alpha} - \frac{h_{pcb}}{2} \pm \sqrt{\frac{h_{pcb}^2}{4} - \frac{l_o h_{pcb}}{\alpha} + \frac{l_o^2}{\alpha^2} - \frac{2l_o h_o}{\alpha}} \quad (4.2)$$

Figure 4.2.: Formulas for trace height  $h_f$  with the substrate bent away from (4.1) or bent into the direction of (4.2) the trace. For derivation, see App. A.1

The same is done for bending the substrate in the direction of the trace, resulting in formula 4.2. Note that  $h_{f+/-}$  for bending upwards (in the direction of the trace) are the same equations as for bending downwards, just with a flipped sign of  $\alpha$ . This is great, positive  $\alpha$  can be used to refer to bending downwards and negative  $\alpha$  for bending upwards. For bending downwards, only  $h_{f-}$  gives plausible values, as  $h_{f+}$  gives values way higher than the radius of the curvature. Therefore  $h_{f-}$  is used to calculate  $h_f$ .

Dividing the resulting trace height  $h_f$  by the original trace height  $h_o$  to show relative change gives us a linear relation between the new trace height and the bending angle. For original trace height  $h_o = 10^{-5}m$ , trace length  $l_o = 5 \times 10^{-2}m$  and PCB height

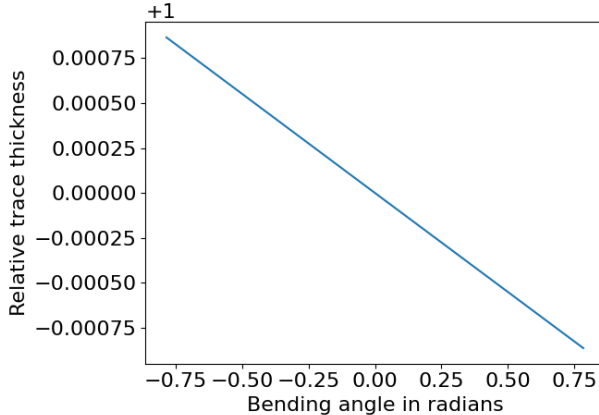


Figure 4.3.: Bent trace thickness  $h_f$  divided by  $h_o$

$h_{pcb} = 10^{-4}m$ , fig. 4.3 shows the linear relation between (relative) trace thickness and bending angle. For example, giving a bending angle of  $0.5rad$ , the resulting trace height is 99.94% of the original trace height. As resistance itself is inversely linear to the cross-section of the conductor, it is also inversely linear to the trace height and therefore linear to the bending angle.

#### 4.1.2. Sensor layout

Strain sensors as described in the model above will measure bending and stretching more in the direction of a trace of conductive ink and less in the orthogonal direction. Therefore strain sensors will perform better when being strained in some directions than in others. The simplest sensor layout would be a single line, changing its resistance when being bent or stretched along its direction. An ever so slightly more complex layout to measure a given area would be  $n$  parallel traces, connected by a few short, perpendicular traces. This layout (shown in Fig. 4.4) concentrates as much parallel trace distance as possible within a given area, maximizing sensitivity in the direction of the longer

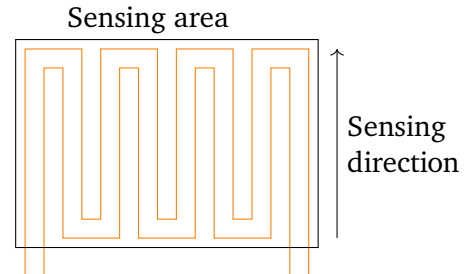


Figure 4.4.: Basic sensor layout

traces. This direction will be called the sensing direction. The area in which effects shall be measured is called the sensing area.

Compared to a single trace into the sensing direction, such a layout, consisting of many traces in the sensing area, makes sure that changes in the sensing area have a larger relative effect than changes to traces outside of the sensing area, for example, in traces leading from a connection point or a reading device to the area, or changes in resistance in connection points.

There are other layouts possible, for example a cross of two conductive traces to measure effects in two directions or a circle to measure independent of the direction of strain, at the cost of multiple parallel traces in the sensing direction. Also, layouts and sensing area can be adapted to specific needs, for example to measure around structures in the fabric or to deeply integrate conductive sensing traces into stretchable circuits. Because conductive traces on a substrate have nearly no restrictions in their layout, this kind of sensors is very freely adaptable to very specific needs.

#### 4.1.3. Integrating the Sensor

Knowing the expected properties of a single printed load cell, a suitable sensing circuit must be designed. The constraints depend on the physical properties and sensing capabilities of the analog-digital converter (ADC) used later on, except for the main goal of measuring the substrate's flexing and stretching. Depending on the behavior of the conductive ink under temperature changes, temperature compensation might be a constraint. If temperature-induced errors are within tolerance, an ADC-internal reference voltage could be used if the chosen ADC offers this functionality.

The most straightforward arrangement would be a voltage divider as in Fig. 4.5a. Such a configuration is sensitive to temperature changes and cannot differentiate between a bent and a stretched substrate. To increase sensitivity, one could replace the constant resistor  $R_0$  with another printed load cell as shown in Fig. 4.5b. This configuration would be temperature-insensitive TODO (Really? U sure, bro?), and  $V_S$  would change in relation to flexing, but not when the substrate is stretched. When the substrate is stretched, the total resistance of both cells would change. However, this would not be measurable at  $V_S$ . Depending on the specific resistance of the conductive ink used, constant resistors in series with  $R_{S1}$  and  $R_{S2}$  may be needed to limit current flow and power consumption if the total trace resistance is too low.

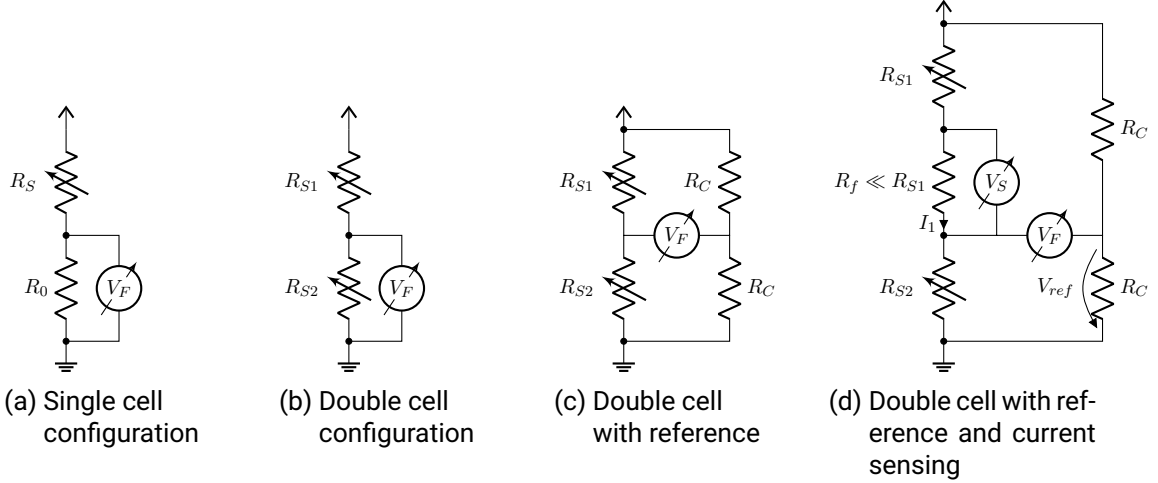


Figure 4.5.: Voltage divider configurations

Using an ADC with a Programmable Gain Amplifier (PGA) reduces the voltage range of the ADC while increasing accuracy. Although this is useful and may be necessary, it reduces the sensing range to less than  $VCC/2$ , which is why a reference voltage of approximately the same level is required. If the ADC doesn't offer such a reference by itself, an external one has to be created, as in Fig. 4.5c.

To measure stretching and flexing separately, the relation of both load cell resistances  $R_{S1}$  and  $R_{S2}$  and the total resistance must be measured. For this, a small fixed resistance  $R_f$  can be put in series with the printed cells, shown in Fig. 4.5d. By measuring the voltage across this resistor, the current flow  $I_1$  and total resistance of both cells can be calculated.

---

## 4.2. Compute Node Design

---

### 4.2.1. Choosing Hardware

#### The Microcontroller

For the microcontroller, an ESP32-S3 was chosen. ESP32 is a widely used microcontroller in embedded systems, as they are a low-cost, low-power SoC with Wi-Fi and Bluetooth capabilities.[16]

The ESP32-S3 uses a dual-core Xtensa LX7 processor, and offers different sleep modes[23], reducing energy consumption down to  $7\mu\text{A}$  in deep sleep mode[11].

#### An Appropriate ACD

In this section, different ADCs are compared. To compare them, an example sensor setup is used for calculation. The parameters of this example sensor can be found in App. B.1. The predicted behavior of the example sensor is shown in Fig. 4.6 and shows a range of about  $\pm 0.3\text{mV}$ .

#### ESP32 internal ADC

The ESP32 ADC does not offer differential measurements. While it has a PGA to measure voltages up to 3.1V, activating this attenuation induces up to 50mV of total error. Therefore, an external ADC has to be used to achieve sufficient accuracy. Even without any error taken into account, the LSB of the ADC spans approximately 0.43mV, which is more than the needed range of around 0.3mV.

#### ADS1115

An immensely popular ADC (at least in the hobbyist community) and low-cost choice is the ADS1115[27] by Texas Instruments. It offers four sensing channels, differential measurements, and a 16-bit resolution, along with a PGA that measures from  $\pm 0.256\text{V}$  (no attenuation) to  $\pm 6.144\text{V}$  (full attenuation). Without attenuation, this equals a LSB range of  $7.8125\mu\text{V}$ , with negligible device-induced noise at sampling rates of  $\leq 64$  samples per second.

A disadvantage of this approach is that it has only four channels and no internal reference voltage, meaning that if a sensor, as shown in Fig. 4.5d, is used, which requires two voltage measurements between three connections, an ADS1115 per sensor would

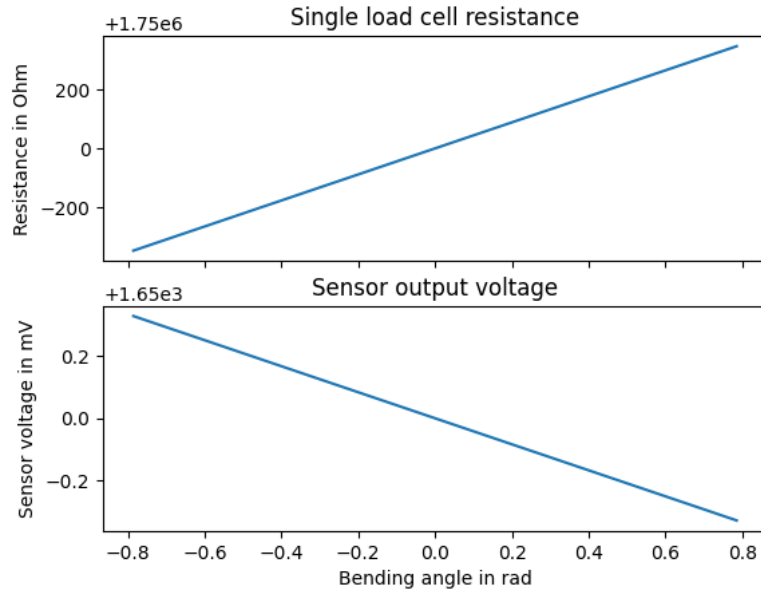


Figure 4.6.: Cell resistance and sensor voltage plotted with parameters from App. B.1 and double cell configuration as in Fig. 4.5b

be needed. One could remove the need for an external reference if no differential, but absolute measurements were taken. This would require a lower PGA setting to measure up to  $VCC/2$ , which would reduce its accuracy, as shown in Fig. 4.7.

**ADS114S08B** Another good fit is the ADS114S08B[1], a 16-bit, 12-channel ADC with an internal 2.5V reference. Due to its reference voltage and 12 channels, up to 6 sensors could be connected to a single ADC chip. While it also features a 16-bit resolution, it offers a higher PGA attenuation. At its highest setting, the ADC reaches a full-scale range of  $\pm 0.020V$  compared to  $\pm 0.256V$  with the ADS1115. This results in a significantly smaller LSB range of  $0.610\mu V$ . Compared to Fig. 4.7, this would just be an orange line on top of a blue one.

The biggest disadvantage of this chip is that it is significantly more complicated compared to the ADS1115. To achieve the high accuracy stated in the datasheet[1], many PCB design factors have to be taken into account, as parasitic inductances, capacitances, and decoupling of differential traces. Nevertheless, due to its many channels, this chip might be the best choice for this use case.

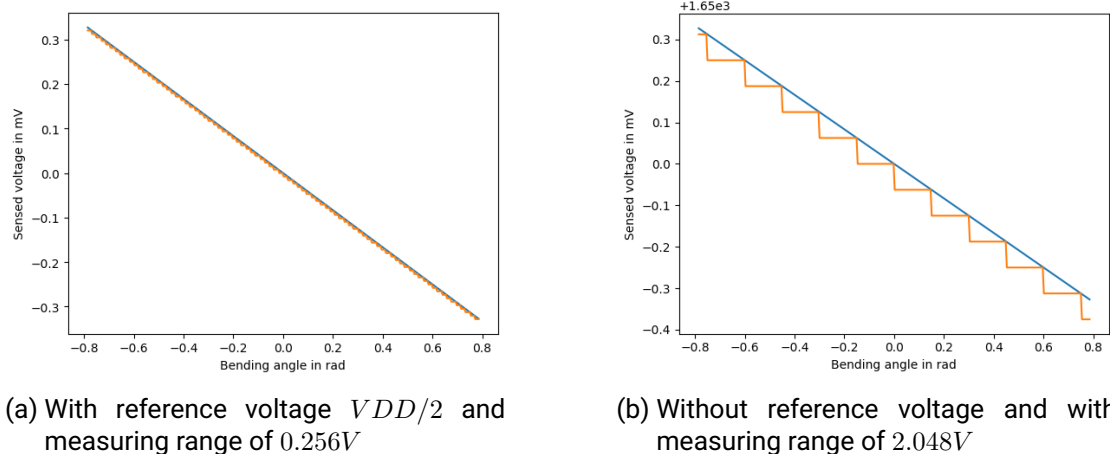


Figure 4.7.: Analog values (blue) and measured values (orange) for ADS1115[27]

### 4.3. A Modular Network

With the sensor designed and the accompanying hardware chosen, we now need to design a network to connect multiple sensors and form a smart fabric. Such a network should support the following fabric criteria:

- **Scalability**  
Making it possible to query a large compound of sensors. Up to a grid of 100x100 ideally
- **Modularity**  
Making it easy to expand the network and add more sensors
- **High resolution in time** Get sensor values at a high frequency

There are many widespread protocols in the DIY electronics area, the most commonly used and supported by the ESP32-S3 being I<sup>2</sup>C, SPI, and UART over wire and WiFi, as well as Bluetooth (BT) and ESP-NOW wireless.

---

### 4.3.1. Wireless Protocols

Wireless protocols typically suffer from two main drawbacks: they consume more power compared to wired protocols, and their scalability is inferior. But in terms of modularity, they outperform wirebound protocols, as no human action or setup is required to connect two or multiple nodes. Also, wireless broadcasts are superior to wire-bound broadcasts. Even in a large grid, each node could easily reach every other node or broadcast a message to be received by all other nodes. With wires, this is not easily achievable without connecting all nodes into a large network, which introduces other problems.

TODO Talk about slower throughput and networking issues due to many parallel wireless connections. There are multiple reasons why a wirebound protocol is used in this work. A wireless protocol would limit scalability in the future, particularly when more nodes are added. Wires used for a protocol don't affect modularity, as power will be distributed through wires as well. Therefore, human action is needed to add or remove nodes anyway. And for the last reason, wired protocols are less dependent on the environment.

### 4.3.2. Wirebound Protocol Candidates

Now for the wired protocols, all the ones already mentioned also suffer problems in this application:

#### **Candidate: I<sup>2</sup>C**

I<sup>2</sup>C (or IIC, for Inter Integrated Circuit) is a half-duplex serial controller-peripheral protocol. The name comes from an umbrella term for more complex components on circuit boards, which are called "Integrated Circuits". I<sup>2</sup>C requires only two wires: one for the clock signal coming from the controller and one for data, which can come from either the controller or the peripheral. Multiple peripherals can be connected to the same bus, and I<sup>2</sup>C uses addresses to determine which peripheral should listen to the sent data. This requires either hardcoded addresses or an address resolution mechanism, which is not a trivial task. Additionally, I<sup>2</sup>C uses 7-bit addresses, resulting in a maximum of  $2^7 = 128$  nodes. Additionally, with a maximum speed of 400kHz (On the ESP32), even ignoring overhead, the data rate is quite low compared to other protocols.

---

### **Candidate: UART**

UART (Universal Asynchronous Receiver/Transmitter) is a full-duplex serial interface with a maximum speed of 5Mbit/s. It uses only two wires and does not suffer from protocol overhead, because it only allows one-to-one connections. Because of that, UART is not scalable and not suited for this use case.

### **Candidate: SPI**

SPI (Serial Peripheral Interface) is a full-duplex serial controller-peripheral protocol, usually used for communication between a microcontroller and its peripherals. With a maximum speed of 80MHz, this eliminates the need for protocol overhead, resulting in a data rate of 2x80Mbit/s, which is significantly faster than other embedded protocols. That's also why it is often used for communication between a microcontroller and its Flash storage, for example, on the microcontroller ESP32-S3, used in this work. SPI needs three wires for the bus itself: One for the clock, and one for data in each direction, coming to and from the controller. Just as I2C, SPI supports multiple peripherals and one controller connected to the bus. To determine which of the connected peripherals should listen to the controller, a CS (Chip-Select) wire is connected from the controller to each peripheral, and the controller uses that wire to notify the peripheral that is supposed to listen or send next. SPI, therefore, is not very scalable: Each SPI bus needs  $3 + n$  wires for  $n$  peripherals, and due to its static role assignment, it is not very flexible.

#### **4.3.3. CAN Bus**

Controller Area Network (CAN, standardized in ISO 11898-1 to ISO 11898-6) is a protocol often used in and developed for the automotive domain. With a maximum speed of 8 Mbit/s, CAN is relatively fast compared to the other protocols listed above. CAN is a multi-master protocol, allowing multiple controlling devices to be connected to the same bus. None of the other buses listed above allows that. Two devices attempting to send data over the SPI bus simultaneously would even result in damage to one of the devices, as a short circuit would occur.

CAN allows multiple devices to transmit simultaneously. One of the main features of CAN is called Carrier Sense Multiple Access/Collision Resolution. This is how it works: The CAN bus can have two states: either recessive (both wires are at the same voltage, usually

2.5V. This state translates to a 1) or dominant (both wires have different voltages, one at 3.5V and one at 1.5V, this state translates to 0). A CAN frame starts with an identifier, either 11 or 29 bits long. This identifier also marks the priority of the frame at the same time. While sending, each sender sends and listens to the bus at the same time. If there is a collision and the frames have different IDs, at some point, one sender tries to send a 1 while the other sends a 0. As 0 decodes the dominant state of the bus, the 0 overwrites the 1. The sender, trying to send the 1, reads a 0 on the bus, knows there is a collision happening, and stops sending. This not only means that it's fine for multiple nodes to send data at the same time, but it also means frames with a lower identifier are prioritized.

The data rate of 1 MBit/s and the voltage levels of the dominant and recessive states are correct for the fast mode of CAN. There is also a slow mode, which should be used with buses over 40m. That makes CAN superior in cable length/data rate over all the other buses mentioned above. SPI supports a higher data rate, but it is not designed to be routed out of a circuit board. Although it is also designed to be used on a circuit board (hence the name), there are records of I2C buses up to 100m long and working, but I2C is inferior to CAN in its data rate.

Up to a length of 40m, the CAN bus supports at least 30 nodes, even more if the electrical conditions are good. To satisfy our scaling goal, multiple CAN buses have to be connected with switch nodes that move messages between them.

Aside from CR, CAN offers another main advantage, especially over SPI: CAN only needs two wires, independent of the number of nodes connected to the bus. That means we only need four wires to connect two nodes: Power, Ground, CAN+, and CAN-.

### **Scaling beyond the network capacity**

As a contrast to CAN, at a controller-peripheral bus, the controller needs to iterate over all the connected peripherals, getting their sensor data. Now, there will be a case where a sensor has not changed its value since the last reading. It still takes the same time to query it. If more sensors are added, the iteration will take longer. And therefore, the resolution in time will become lower. It is a trade-off between querying frequency and the number of nodes being queried, constrained by the data rate of the connecting network.

Now using CAN, this is not necessary. As a message identifier and therefore priority, the inverted change in sensor result since the last successfully sent frame is chosen. Inverted because lower values indicate a higher priority, but high changes should be prioritized.

If a packet fails to be sent, each compute node resends the packet or updates its priority if a new sensor value was read in the meantime.

This results in the most relevant messages being sent at the highest frequency. If the bus has enough capacity for all sensor values, all of them will be sent. If not, the least important messages will be omitted. This is really useful for the goal of scalability. The network can be scaled, no matter its throughput. Monitoring the lowest received priority in a given time frame can give an approximation of whether the bus capacity is enough for the number of nodes and the sensor update frequency. If the lowest priority received was a change at or near 0, nearly no information is expected to be lost. If not, it is to be expected that, while being the least important, some information is lost, and maybe the sensor update frequency should be reduced.

### **Drawbacks of CAN**

CAN has one major drawback: its topology. As CAN works by the sender pulling the bus into the dominant state and the bus pulling itself back into the recessive state, there are strict rules on how to pull the bus back into its recessive state. For longer high-speed CAN buses, this allows only a linear topology. No junctions are allowed, while stubs have to be kept as short as possible. At both ends, there will be a  $120\Omega$  resistor pulling the two bus lines back together into the recessive state.

For smaller or low-speed buses, a star topology is used with one central hub and the bus splitting in multiple directions. Either the bus is only terminated at the hub with a  $60\Omega$  resistor, or at the ends with a higher resistance. The issue with too many arms without termination resistors is that the signal might reflect at the ends and transmit back along the bus, causing glitches. But with too many terminations, the sender might not be able to transmit its signal along the whole bus, as the capability of the sender to pull the bus into the dominant state is outweighed by the termination resistors pulling against it.

### **CAN on the ESP32-S3**

The ESP32-S3 implements something it calls TWAI (Two-Wire Automotive Interface). TWAI is the same as CAN in a basic version with 1MBit/s throughput, leaving some features unsupported. The ESP32-S3 chip implements the controller part of a CAN network. Controller in this case is not related to the term "Controller-Peripheral", but indicates it is missing a transceiver. Basically, the chip can do the logic and handle a digital output

and a digital input. But the physical part of CAN requires the voltages of two wires to be pulled up and down, at a given rate, and handling the shape of the slope of these voltage changes. For this part, another chip is needed - a dedicated CAN transceiver. These can be found in many versions on the consumer market. The implementation below uses a chip by Texas Instruments, the SN65HVD230[24].

## 5. Implementation

---

For testing and a proof of concept, we aimed for a first compute node and sensor implementation. These experimental sensors would be the first real project on the planar printer we aim to use for such projects, a NOVA printer by Voltera[18]. We also aimed to validate the model in section 4.1.1 with these sensors and further test their properties, durability, and the repeatability of their stretching.

### 5.1. First Physical Compute Node

---

The first iteration of the compute module was built to test the capabilities of the ADS114[27], the first experimental sensors, and the practicability of the different circuits discussed in section 4.1.3

The compute node consists of 3 main sectors:

1. Computation
2. Measurement/Analog domain
3. Communication

#### Computation

We already chose an ESP32-S3 as the main microcontroller in Section 4.2.1. As designing peripherals for the ESP32-S3 IC itself would require a more complex design and soldering, a COTS ESP32-S3-Tiny[4] module, designed by Waveshare, was chosen. It offers a very small integration of the ESP32-S3 IC combined with a FFC flex cable connector for USB connection to the device, up to 34 usable GPIOs, and an on-board addressable LED, which makes it the best candidate for our purpose.

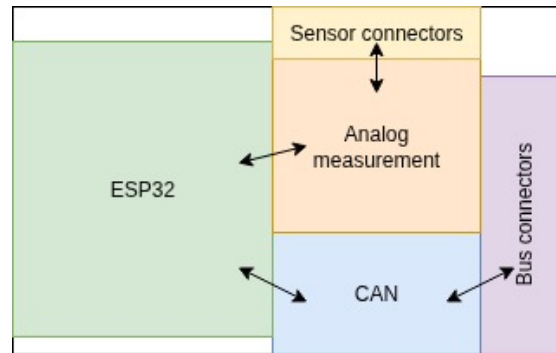


Figure 5.1.: Broad layout of the PCB, arrows indicate traces connecting areas

It also features a small integrated antenna, which leaves us with the option to choose communication over the air.

### Measurement/Analog Domain

An ADS114 was chosen as the most fitting ADC for performing the measurements, as discussed in section 4.2.1. Of its 12 inputs, only 4 are usable on this test board to keep the board as a whole simpler and smaller. In its datasheet[1], it states the need for divided analog and digital domains, which can still share a connected ground.

In the digital domain, the ADS114 communicates mainly over a SPI interface and a few extra status/command pins. The SPI bus is connected directly to the ESP32-S3-Tiny. In the analog domain, each input needs a bypass capacitor to ground. For each differential input, each differential pair has to be decoupled by a capacitor as well.

The whole measuring circuitry can be found on its own sub-schematic in App. C.

### Communication

As the ESP32 only has a CAN controller integrated and lacks a transceiver, an external transceiver is needed, and the already mentioned SN65HVD230[24] is integrated into the circuit as such a CAN transceiver. It gets a digital input signal from the ESP32 that controls when the transceiver tries to pull the CAN lines into the dominant state. In parallel, the transceiver translates the current state of the CAN bus into a digital signal

that it sends to the ESP32. This means the ESP32 can send its data to the transceiver and, at the same time, monitor the bus to watch for transmit collisions (this is called Carrier Sense Multiple Access, explained in Sec. 4.3.3).

The circuitry around the SN65HVD230 can be found in the schematic in App. C. As stated in the datasheet of the SN65HVD230, some bypass (filter out high frequencies) and decoupling (smoothen out supply voltage) capacitors are added as well as two  $0\Omega$  resistors to limit current between the microcontroller and the SN65HVD230. In this schematic the CAN bus termination can be seen as well, consisting of  $120\Omega$  in total between both bus lines with a bypass capacitor in the middle.

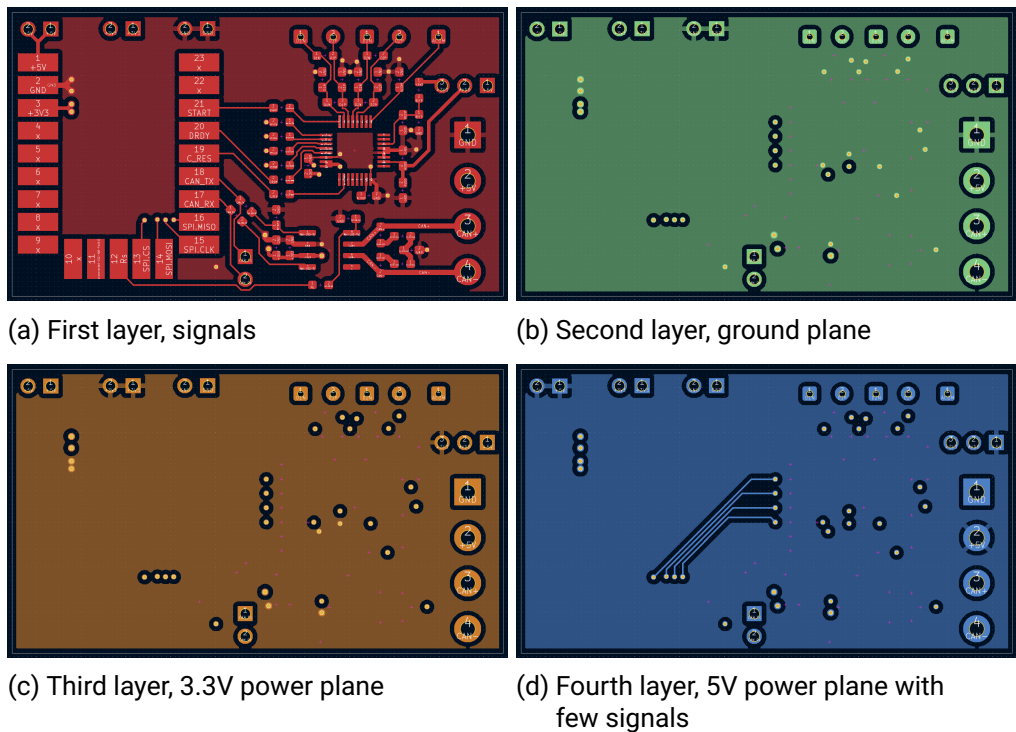


Figure 5.2.: Gerber views of all four copper layers

### 5.1.1. PCB Design

Coming from the schematics, now all the components have to be assigned to a physical footprint (e.g. which size of resistors to use), a broad layout has to be chosen, components placed and then traces routed (for people new to PCB design: routing traces means using copper "tracks", called traces, to connect things that should be connected. This can get quite complicated on more complex boards).

The broad layout is shown in Fig. 5.1. The actual PCB can be seen in Fig. 5.2. It consists of four copper layers, the first (and upper, therefore outer) layer acts as a signal layer, connecting most of the footprints placed on top of it. The filled areas on the first layer are connected to GND. The second layer is used as a ground plane, which means it is filled with copper and connected to GND. This creates a low-impedance return path for currents and is necessary for the ADS114 ADC. The third layer is a power plane, similar to the ground plane, it is filled with copper but connected to +3.3V, just to make it easier to supply +3.3V as many components need to be connected to it. The bottom layer hosts some signals that do not fit on the upper layer and also acts as a +5V power plane.

All four layers stacked can be seen in Fig. 5.3, as well as a rendered view of the PCB including its components and a photo of the finished physical PCB after soldering.

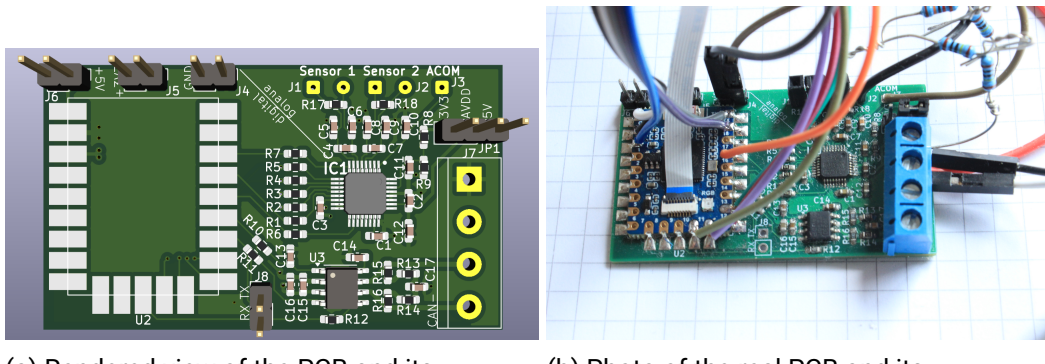


Figure 5.3.: View of the rendered model of the compute node board and a photo

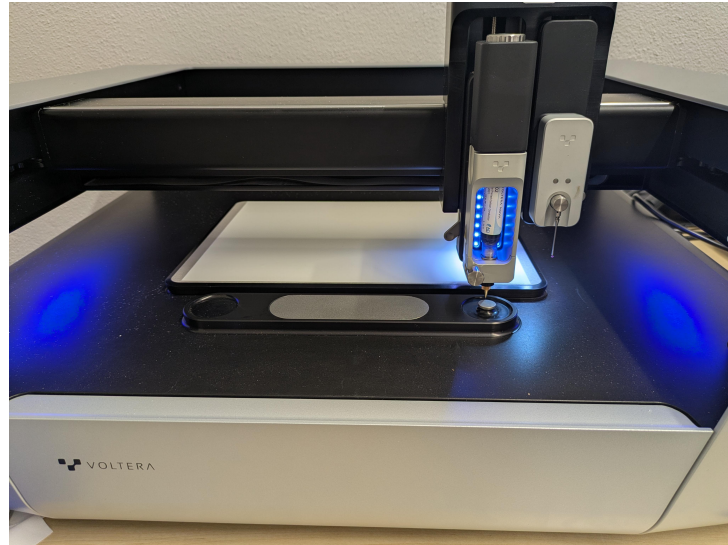


Figure 5.4.: Voltera NOVA

---

## 5.2. Prototyping a sensor

---

### 5.2.1. Voltera NOVA

To build a physical sensor, an inkjet printer was used to print conductive ink onto a stretchable substrate. The printer used here is the Voltera NOVA[18], a picture is shown in Fig. 5.4 TODO: Besseres Bild machen. Launching in 2022, the NOVA offers the ability to print with many different inks on many substrates. For soft substrates, it has a vacuum table so the substrate is fixed, and for hard substrates, screws can be used to hold them in place.

NOVA offers to print up to four layers in a design with multiple different materials per layer, if needed. Combining conductive and insulating inks leads to a high degree of flexibility in the designs printed. Voltera sells a few inks themselves, but any compatible ink can be filled into syringes and fed to the printer. For sensors in this paper, an ink named SC1502[22], produced by ACI Materials, is used.

While many substrates are usable, for the sensors in this work, TPU was used. TPU is very stretchable and easily bendable, there are samples shipped with the printer, and the ink used provides the best adhesion to TPU. There are also different nozzles available and

we tried different sizes and ended up using mostly the bigger  $225\mu\text{m}$  nozzles as printing is easier as fewer lines are needed due to their higher width, while the level of detail producable with them is still high enough for this work.

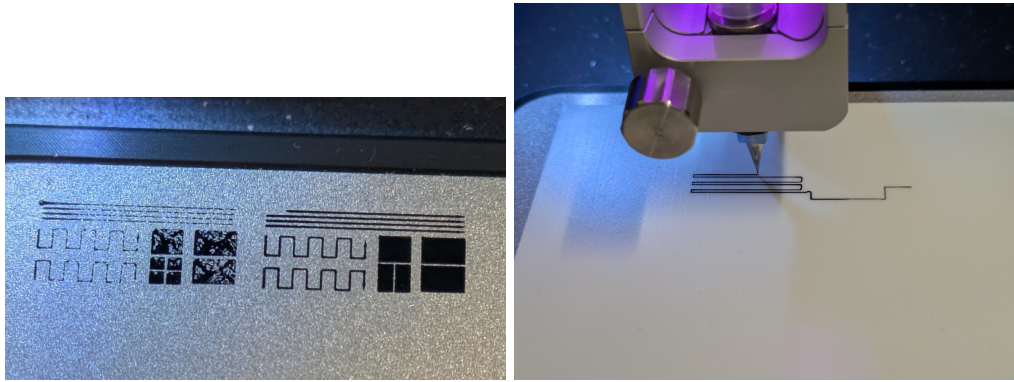


Figure 5.5.: Pictures of NOVA

### Printing Procedure

Before the desired shape can be printed, if the ink to be used is new or the nozzle was changed a calibration has to be done to get the right dispense pressure for the print. This procedure starts by increasing pressure until ink flows out of the nozzle and then printing a test shape on its calibration plate in front of the build plate. The shape and the difference between uncalibrated and calibrated can be seen in Fig. 5.5a where the left shape is not calibrated while the right one is.

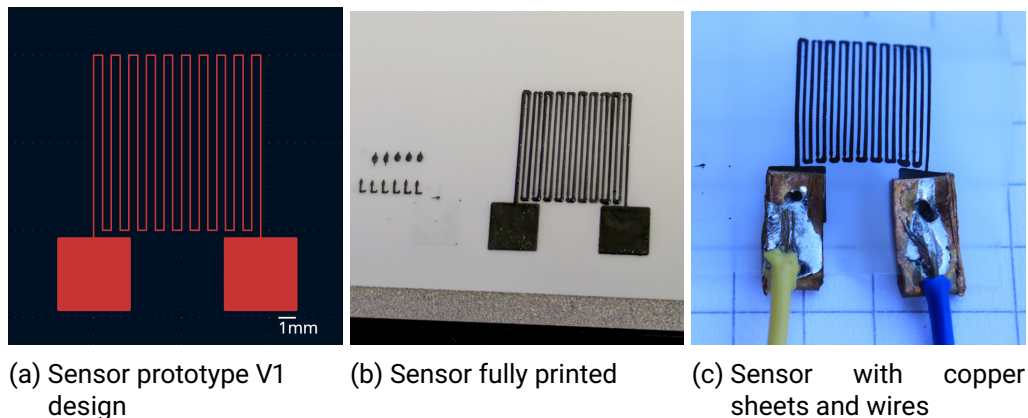
When starting the actual print, the substrate can be mounted, and the desired shape can be loaded to the NOVA. It will then start by homing its calibration probe and measuring the surface heights of the calibration plate and the print area. After this is finished, it will again print a few lines onto the calibration plate to confirm correct calibration settings and then start printing the actual shape as seen in Fig. 5.5b.

After the printing is finished, the ink has to be cured by heating it up to. It is recommended to cure the ink in an oven. The datasheet of the ink used (see App. E.1) states recommends heating over  $\geq 120^\circ\text{C}$ . We used the hot plate of a Voltera V-One[30] to cure, as this method is also proposed by Voltera, and we have a V-One in our lab.

As this is the first time this printer is used in our lab, a risk assessment was created, it is attached in App. D.

### 5.2.2. Sensor V1

The first prototype was a simple sensor with two enlarged pads for attaching wires; the design Gerber file is shown in 5.6a. The shown Gerber file was used to print the sensor with the NOVA on a  $100\mu\text{m}$  thick TPU sheet. Fig. 5.5b and 5.6b show the sensor during and after printing, with a failed printing attempt to the left of the sensor in Fig. 5.6b.



Looking at the results and measuring the resistance of the sensor, which came out to be  $600\text{k}\Omega$ , made it clear that for the next iteration, a higher trace thickness is needed <TODO>. In Fig. 5.6b, it can be observed that the printer was not precise enough, as sensor lines touch in spots where they should not, creating a short circuit over some part of the sensor. To precisely measure bending and stretching, the sensor had to be kept in place to be bent at the sensing area and not the contacts. As the pads were very close to the sensing area, this was hard to achieve.

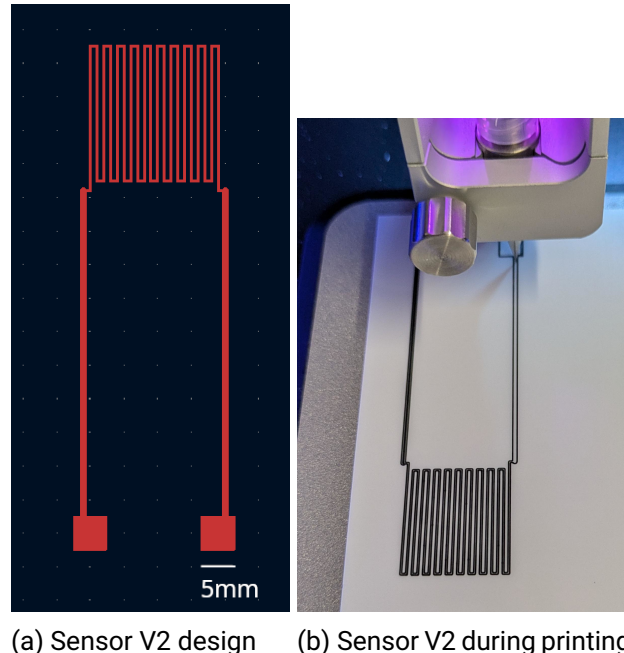
The soft-hard problem turned out to be harder to solve than imagined. As discussed in the literature as well, connecting a flexible body to a rigid body requires some type of soft-hard interface to connect physically and conduct electricity from the flexible part to the rigid one and vice versa. Some possible solutions on the molecule-, nano-, or microscale are already documented[6], as well as solutions using two polymers with different rigidness to create a bonding polymer with a stretchability gradient[17]. But all these solutions are beyond the scope of this work. That's why, for a first attempt, it was

tried to wrap a copper sheet around the edge of the sensor near the contacts and make it touch the contacts on the upper side and the substrate on the lower side in the hope that friction held it in place after it was hammered shut, the result can be seen in Fig. 5.6c. But the friction was not enough to keep the sensor from slipping out of it, so the copper sheet was deformed in the middle to increase friction. Still, the sensor could move too much and was about to slip out of its contact. As the sensor contacts were damaged by the deformed sheet, further investigation into solving this problem had to be postponed to the second version of the sensor.

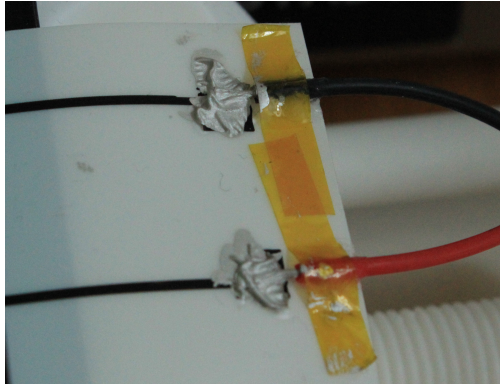
As this sensor was too small to attach it somewhere, no methodical measurements were made. But looking at the resistance of the sensor while changing its shape showed small changes in resistance.

### 5.2.3. Sensor V2

**The second prototype** tried to solve problems detected with the first prototype. It still only consisted of one sensing cell on one side of the substrate. A screenshot of the design file is shown in Fig. 5.7a, pictures during printing and curing in Fig. 5.7b and Fig. ??.



(a) Sensor V2 design      (b) Sensor V2 during printing



(a) Wires connected to Sensor V2 with ad-



(b) Four wires, connected to four pads of Sensor V3

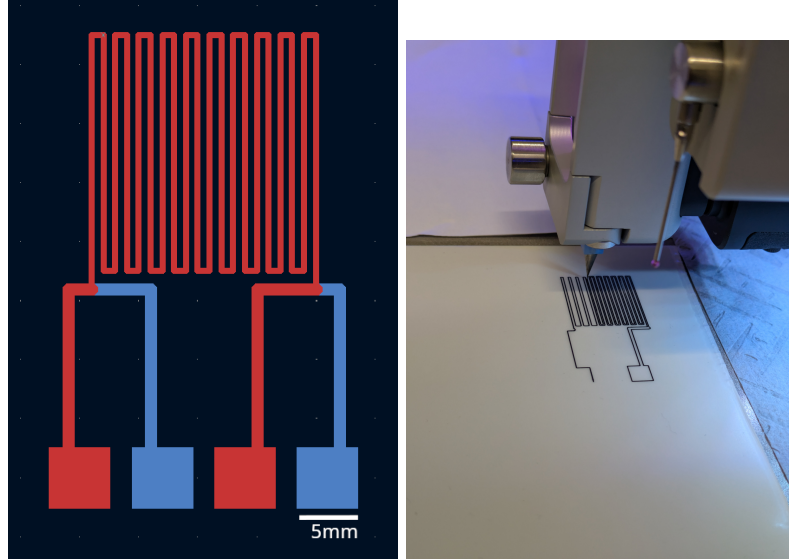
To solve the soft-hard problem on the second prototype, conductive adhesive tape was tried first, but it didn't conduct enough electricity to act as a connector. The second attempt was conductive glue. This glue is made from silver particles, similar to conductive inks used in inkjet printing technologies. Using this, two wires were glued to the pads of the sensor. To reduce stress on the glue, the wires were fixed to the TPU substrate with adhesive tape and non-conductive glue. Measuring the resistance of the sensor with and without the glue reveals no measurable resistance being added by the conductive glue.

The longer distance between the pads and the sensing area of the sensor allowed it to be locked into position with a clamp and perform some more precise measurements. First, a clamp was designed, then mounting plates with different bending angles.

#### 5.2.4. Sensor V3

The Sensor V2 showed that the sensor reacts to stretching and bending and acted as a PoC for further development. Sensor V3 comes with 3 new features:

1. It is a dual-layer implementation, having a sensing element on both sides of the substrate
2. The substrate consists of two TPU sheets, making it thicker and the sensor more responsive to bending
3. Shorter leads between the connection pads and the sensing area



(a) Gerber view of the Sensor V3 with two layers (red and blue) (b) One side of Sensor V3 during printing

A view of the sensor design files can be found in Fig. 5.9a. Having two layers allowed the sensor to be connected in a double cell configuration (as shown in Fig. 4.5), as the sensor now has two changing sensing elements to be used as  $R_{S1}$  and  $R_{S2}$ .

Using two TPU sheets was a necessity in the manufacture of the sensor. The TPU sheets used come on a more rigid substrate for printing. After printing onto the first side of the TPU sheet, the rigid substrate has to be removed, and after curing, the TPU sheet has to be put onto the printer with the side up to which the substrate was attached. Printing on this side is very hard, as the ink does not bond to the TPU nearly as well as on the other side. Directly after curing, or sometimes after the first stretching, visible cracks formed in the ink on this side. These cracks resulted in the ink on this side not conducting electricity anymore after stretching it for a few millimeters, while the ink on the other side behaved as expected, changing linearly. Therefore, both layers of the sensor are printed on two different sheets of TPU, and the sheets are fused together by heating them up.

The shorter leads between the sensing area and the connection pads, combined with printing two layers of TPU, result in a resistance of around  $200k\Omega$ , which is 40% of the resistance of the Sensor V2, which had around  $500k\Omega$ . Less resistance means a higher current flow, which makes measuring the current flow more accurate.

Just as in Sensor V2, wires are attached to this sensor using a conductive glue, which does not add a measurable amount of resistance. To minimize stress on the conductive glue, the wires are held in place by non-conductive glue and some tape. Due to having two sensing elements, one on each layer, the sensor now has four connection pads and therefore four wires connected. Two pads are on each side of the sensor. Near the connection pads of one side of the sensor, two holes are punched into the TPU to allow the wires to pass to the other side. A photo of the connected wires is present in Fig. ??

### 5.2.5. Manufacturing pitfalls

#### Heating to the right temperature



Figure 5.10.: What a difference 100°C can make

One Sensor V2 was the victim of a typo in the temperature field of the curing hot plate. After printing, instead of the desired 120°C, the sensor was heated to around 220°C, resulting in a complete meltdown of ..the sensor, of course.

#### Brittle ink

---

## 6. Results and Analysis

---

To analyze the static capabilities of our fabric, we first evaluated the inkjet-printed sensors and conducted multiple tests to be able to calculate their linearity, sensitivity, hysteresis, repeatability, and resolution[21].

---

### 6.1. Sensor prototype V2

---

For this purpose,



---

## 7. Conclusion

---

e

---

## 8. Discussion

---

Might in the future use a bigger network of CAN buses fused together and arranged in a topology such as the one mentioned in[3].

## Bibliography

---

- [1] *ADS114S08B data sheet, product information and support | TI.com*. URL: <https://www.ti.com/product/ADS114S08B> (visited on 03/10/2025).
- [2] Arnesh K. Bose et al. “Screen-Printed Strain Gauge for Micro-Strain Detection Applications”. In: *IEEE Sensors Journal* 20.21 (Nov. 2020). Conference Name: IEEE Sensors Journal, pp. 12652–12660. ISSN: 1558-1748. doi: 10.1109/JSEN.2020.3002388. URL: <https://ieeexplore.ieee.org/document/9117025/?arnumber=9117025> (visited on 01/23/2025).
- [3] Umut Can Çabuk, Mustafa Tosun, and Orhan Dagdeviren. “MAX-Tree: A Novel Topology Formation for Maximal Area Coverage in Wireless Ad-Hoc Networks”. In: *IEEE/ACM Transactions on Networking* 30.1 (Feb. 2022), pp. 162–175. ISSN: 1558-2566. doi: 10.1109/TNET.2021.3110675. URL: <https://ieeexplore.ieee.org/document/9542954> (visited on 07/14/2025).
- [4] *ESP32-S3-Tiny - Waveshare Wiki*. URL: <https://www.waveshare.com/wiki/ESP32-S3-Tiny> (visited on 05/17/2025).
- [5] Chonghui Fan et al. “Dynamically Tunable Subambient Daytime Radiative Cooling Metafabric with Janus Wettability”. In: *Advanced Functional Materials* 33.29 (2023). \_eprint: <https://advanced.onlinelibrary.wiley.com/doi/pdf/10.1002/adfm.202300794>, p. 2300794. ISSN: 1616-3028. doi: 10.1002/adfm.202300794. URL: <https://onlinelibrary.wiley.com/doi/abs/10.1002/adfm.202300794> (visited on 07/14/2025).
- [6] Shu Gong et al. “Multiscale Soft–Hard Interface Design for Flexible Hybrid Electronics”. In: *Advanced Materials* 32.15 (2020). \_eprint: <https://advanced.onlinelibrary.wiley.com/doi/pdf/10.1002/adma.201902278>, p. 1902278. ISSN: 1521-4095. doi: 10.1002/adma.201902278. URL: <https://onlinelibrary.wiley.com/doi/abs/10.1002/adma.201902278> (visited on 06/17/2025).

- [7] Ahmed Hassabo et al. "SMART Wearable Fabric using Electronic Textiles – A Review". In: *Journal of Textiles, Coloration and Polymer Science* 0.0 (Dec. 31, 2022). Publisher: Egypt's Presidential Specialized Council for Education and Scientific Research, pp. 0–0. ISSN: 2682-1958. doi: 10.21608/jtcps.2022.181611.1148. URL: [https://jtcps.journals.ekb.eg/article\\_277371.html](https://jtcps.journals.ekb.eg/article_277371.html) (visited on 07/14/2025).
- [8] Ahmed G. Hassabo et al. "SMART Wearable Fabric using Electronic Textiles – A Review". In: *Journal of Textiles, Coloration and Polymer Science* 20.1 (June 1, 2023). Publisher: National Information and Documentation Centre (NIDOC), Academy of Scientific Research and Technology( ASRT), pp. 29–39. ISSN: 2682-2024. doi: 10.21608/jtcps.2022.181611.1148. URL: [https://jtcps.journals.ekb.eg/article\\_277371.html](https://jtcps.journals.ekb.eg/article_277371.html) (visited on 07/13/2025).
- [9] Robert Herbert, Hyo-Ryoung Lim, and Woon-Hong Yeo. "Printed, Soft, Nanostructured Strain Sensors for Monitoring of Structural Health and Human Physiology". In: *ACS Applied Materials & Interfaces* 12.22 (June 3, 2020). Publisher: American Chemical Society, pp. 25020–25030. ISSN: 1944-8244. doi: 10.1021/acsami.0c04857. URL: <https://doi.org/10.1021/acsami.0c04857> (visited on 07/14/2025).
- [10] Po-Chun Hsu et al. "Personal Thermal Management by Metallic Nanowire-Coated Textile". In: *Nano Letters* 15.1 (Jan. 14, 2015). Publisher: American Chemical Society, pp. 365–371. ISSN: 1530-6984. doi: 10.1021/nl5036572. URL: <https://doi.org/10.1021/nl5036572> (visited on 08/31/2025).
- [11] [https://www.espressif.com/sites/default/files/documentation/esp32-s3\\_datasheet\\_en.pdf](https://www.espressif.com/sites/default/files/documentation/esp32-s3_datasheet_en.pdf). URL: [https://www.espressif.com/sites/default/files/documentation/esp32-s3\\_datasheet\\_en.pdf](https://www.espressif.com/sites/default/files/documentation/esp32-s3_datasheet_en.pdf) (visited on 02/17/2025).
- [12] Yang Huang et al. "A shape memory supercapacitor and its application in smart energy storage textiles". In: *Journal of Materials Chemistry A* 4.4 (Jan. 20, 2016). Publisher: The Royal Society of Chemistry, pp. 1290–1297. ISSN: 2050-7496. doi: 10.1039/C5TA09473A. URL: <https://pubs.rsc.org/en/content/articlelanding/2016/ta/c5ta09473a> (visited on 07/14/2025).
- [13] Leqi Lei et al. "Recent Advances in Thermoregulatory Clothing: Materials, Mechanisms, and Perspectives". In: *ACS Nano* 17.3 (Feb. 14, 2023). Publisher: American Chemical Society, pp. 1803–1830. ISSN: 1936-0851. doi: 10.1021/acsnano.2c10279. URL: <https://doi.org/10.1021/acsnano.2c10279> (visited on 07/14/2025).

- [14] Xiuqiang Li, Wanlin Guo, and Po-Chun Hsu. "Personal Thermoregulation by Moisture-Engineered Materials". In: *Advanced Materials* 36.12 (2024). \_eprint: <https://advanced.onlinelibrary.wiley.com/doi/pdf/10.1002/adma.202209825>, p. 2209825. issn: 1521-4095. doi: 10.1002/adma.202209825. url: <https://onlinelibrary.wiley.com/doi/abs/10.1002/adma.202209825> (visited on 07/14/2025).
- [15] Sida Luo et al. "CNT Enabled Co-braided Smart Fabrics: A New Route for Non-invasive, Highly Sensitive & Large-area Monitoring of Composites". In: *Scientific Reports* 7.1 (Mar. 8, 2017). Publisher: Nature Publishing Group, p. 44056. issn: 2045-2322. doi: 10.1038/srep44056. url: <https://www.nature.com/articles/srep44056> (visited on 07/07/2025).
- [16] Alexander Maier, Andrew Sharp, and Yuriy Vagapov. "Comparative analysis and practical implementation of the ESP32 microcontroller module for the internet of things". In: *2017 Internet Technologies and Applications (ITA)*. 2017 Internet Technologies and Applications (ITA). Sept. 2017, pp. 143–148. doi: 10.1109/ITECHA.2017.8101926. url: <https://ieeexplore.ieee.org/document/8101926> (visited on 02/06/2025).
- [17] Naoji Matsuhisa et al. "Printable elastic conductors with a high conductivity for electronic textile applications". In: *Nature Communications* 6.1 (June 25, 2015). Publisher: Nature Publishing Group, p. 7461. issn: 2041-1723. doi: 10.1038/ncomms8461. url: <https://www.nature.com/articles/ncomms8461> (visited on 06/17/2025).
- [18] NOVA - A Flexible and Printed Electronics Platform | Voltera. url: <https://www.voltera.io/products/nova> (visited on 05/18/2025).
- [19] Stanley C. Obilikpa et al. "Scalable Plug-and-Play Robotic Fabrics Based on Kilobot Modules". In: *IEEE Robotics and Automation Letters* 10.7 (July 2025), pp. 6832–6839. issn: 2377-3766. doi: 10.1109/LRA.2025.3568313. url: <https://ieeexplore.ieee.org/document/10993294> (visited on 07/09/2025).
- [20] Federico Pratissoli et al. "Coherent movement of error-prone individuals through mechanical coupling". In: *Nature Communications* 14.1 (July 18, 2023). Publisher: Nature Publishing Group, p. 4063. issn: 2041-1723. doi: 10.1038/s41467-023-39660-6. url: <https://www.nature.com/articles/s41467-023-39660-6> (visited on 07/15/2025).
- [21] Xue Qi et al. "Flexible Strain Sensors Based on Printing Technology: Conductive Inks, Substrates, Printability, and Applications". In: *Materials* 18.9 (Jan. 2025). Number: 9 Publisher: Multidisciplinary Digital Publishing Institute, p. 2113. issn:

- 1996-1944. doi: 10.3390/ma18092113. URL: <https://www.mdpi.com/1996-1944/18/9/2113> (visited on 06/17/2025).
- [22] *SC1502 Carbon Filled Conductive Ink | ACI Materials*. May 20, 2023. URL: <https://www.acimaterials.com/sc1502/> (visited on 08/11/2025).
- [23] *Sleep Modes - ESP32-S3 - — ESP-IDF Programming Guide v5.4 documentation*. URL: [https://docs.espressif.com/projects/esp-idf/en/v5.4/esp32s3/api-reference/system/sleep\\_modes.html](https://docs.espressif.com/projects/esp-idf/en/v5.4/esp32s3/api-reference/system/sleep_modes.html) (visited on 02/17/2025).
- [24] *SN65HVD230 data sheet, product information and support | TI.com*. URL: <https://www.ti.com/product/SN65HVD230> (visited on 08/08/2025).
- [25] Hamid Souri et al. “Wearable and Stretchable Strain Sensors: Materials, Sensing Mechanisms, and Applications”. In: *Advanced Intelligent Systems* 2.8 (2020). \_eprint: <https://advanced.onlinelibrary.wiley.com/doi/pdf/10.1002/aisy.202000039>, p. 2000039. ISSN: 2640-4567. doi: 10.1002/aisy.202000039. URL: <https://onlinelibrary.wiley.com/doi/abs/10.1002/aisy.202000039> (visited on 07/14/2025).
- [26] H.Z. Tan, L.A. Slivovsky, and A. Pentland. “A sensing chair using pressure distribution sensors”. In: *IEEE/ASME Transactions on Mechatronics* 6.3 (Sept. 2001). Conference Name: IEEE/ASME Transactions on Mechatronics, pp. 261–268. ISSN: 1941-014X. doi: 10.1109/3516.951364. URL: <https://ieeexplore.ieee.org/document/951364> (visited on 01/06/2025).
- [27] Texas Instruments. *ADS1115*. 2018. URL: <https://www.ti.com/product/ADS1115>.
- [28] Mustafa Tosun et al. “CoRMAC: A Connected Random Topology Formation With Maximal Area Coverage in Wireless Ad-Hoc Networks”. In: *IEEE Internet of Things Journal* 10.14 (July 2023), pp. 12379–12392. ISSN: 2327-4662. doi: 10.1109/JIOT.2023.3246000. URL: <https://ieeexplore.ieee.org/document/10049747> (visited on 07/14/2025).
- [29] Tran Quang Trung and Nae-Eung Lee. “Recent Progress on Stretchable Electronic Devices with Intrinsically Stretchable Components”. In: *Advanced Materials* 29.3 (2017). \_eprint: <https://advanced.onlinelibrary.wiley.com/doi/pdf/10.1002/adma.201603167>, p. 1603167. ISSN: 1521-4095. doi: 10.1002/adma.201603167. URL: <https://onlinelibrary.wiley.com/doi/abs/10.1002/adma.201603167> (visited on 06/17/2025).
- [30] *V-One - PCB Printer | 4-in-1 Desktop Electronics Printing Solutions*. Voltera Inc. URL: <https://www.voltera.io/products/v-one> (visited on 08/11/2025).

- 
- 
- [31] Xuping Wu et al. “Ultra-Robust and Sensitive Flexible Strain Sensor for Real-Time and Wearable Sign Language Translation”. In: *Advanced Functional Materials* 33.36 (2023). \_eprint: <https://advanced.onlinelibrary.wiley.com/doi/pdf/10.1002/adfm.202303504>, p. 2303504. issn: 1616-3028. doi: 10.1002/adfm.202303504. url: <https://onlinelibrary.wiley.com/doi/abs/10.1002/adfm.202303504> (visited on 07/14/2025).
  - [32] Michelle C. Yuen, R. Adam Bilodeau, and Rebecca K. Kramer. “Active Variable Stiffness Fibers for Multifunctional Robotic Fabrics”. In: *IEEE Robotics and Automation Letters* 1.2 (July 2016), pp. 708–715. issn: 2377-3766. doi: 10.1109/LRA.2016.2519609. url: <https://ieeexplore.ieee.org/document/7386608> (visited on 07/14/2025).

---

## A. Formulas and derivations

---

---

### A.1. Trace height in relation to bending angle

---

$$\begin{aligned} A &= \frac{\alpha}{2}((r + \frac{h_{pcb}}{2} + h_f)^2 - (r + \frac{h_{pcb}}{2})^2) \\ &= \frac{\alpha h_f^2}{2} + \frac{\alpha h_f h_{pcb}}{2} + l_o h_f \\ 0 &= h_f^2 + h_f(\frac{2l_o}{\alpha} + h_{pcb}) - \frac{2l_o h_o}{\alpha} \\ h_{f+/-} &= -\frac{l_o}{\alpha} - \frac{h_{pcb}}{2} \pm \sqrt{\frac{h_{pcb}^2}{4} + \frac{l_o h_{pcb}}{\alpha} + \frac{l_o^2}{\alpha^2} + \frac{2l_o h_o}{\alpha}} \end{aligned} \quad (\text{A.1})$$

---

## B. Example values

---

---

### B.1. Example sensor setup

---

Conductor volume resistivity  $< 0.5\Omega \cdot cm$

This is the volume resistivity of SC1502, a stretchable ink produced by ACI[22].

$\text{trace\_height} = 6\mu m$

Lower bound stated by SC1502 datasheet for cured thickness.

$$s_l = 20cm$$

$$t_w = 100\mu m$$

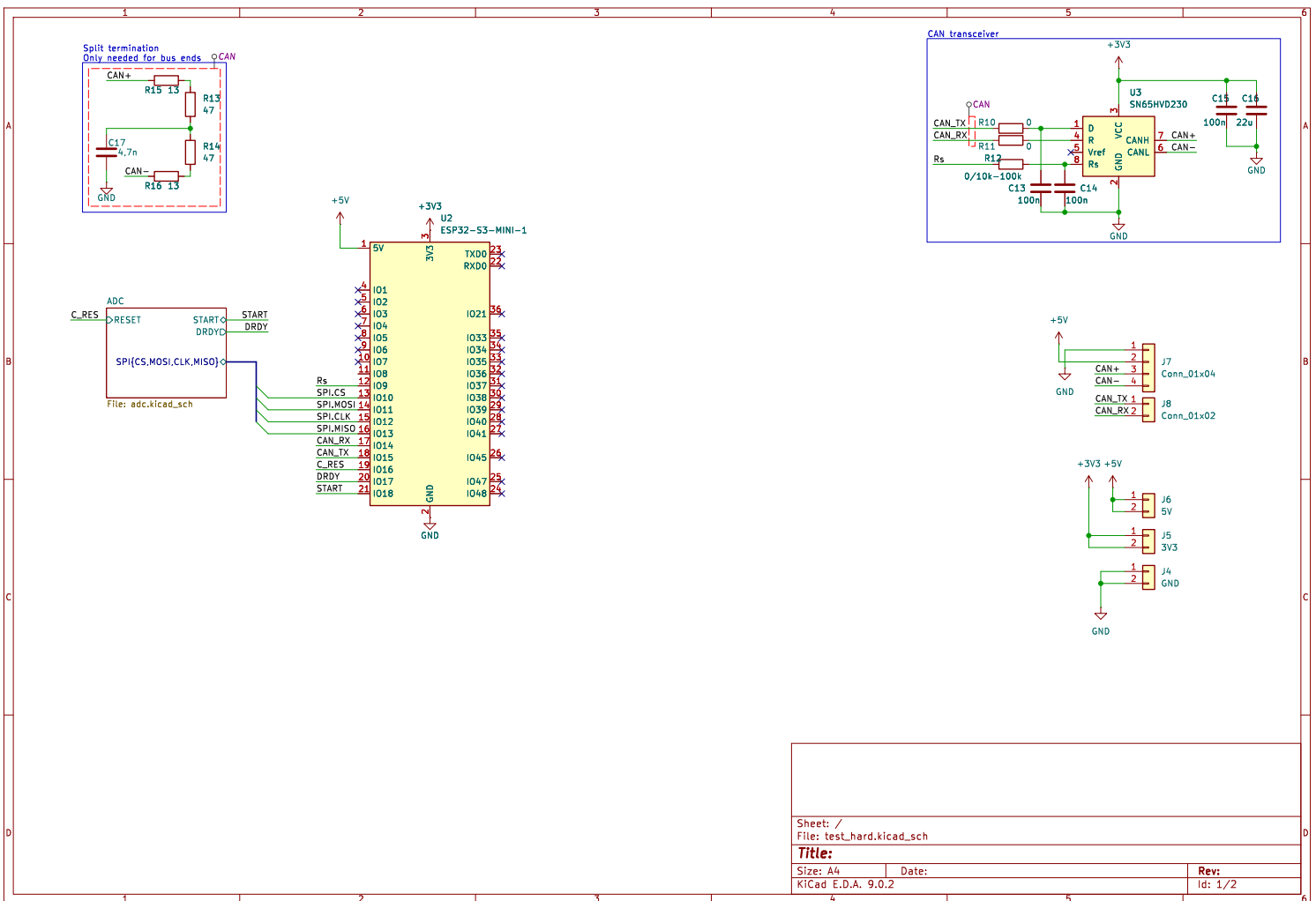
$$s_w = 1cm$$

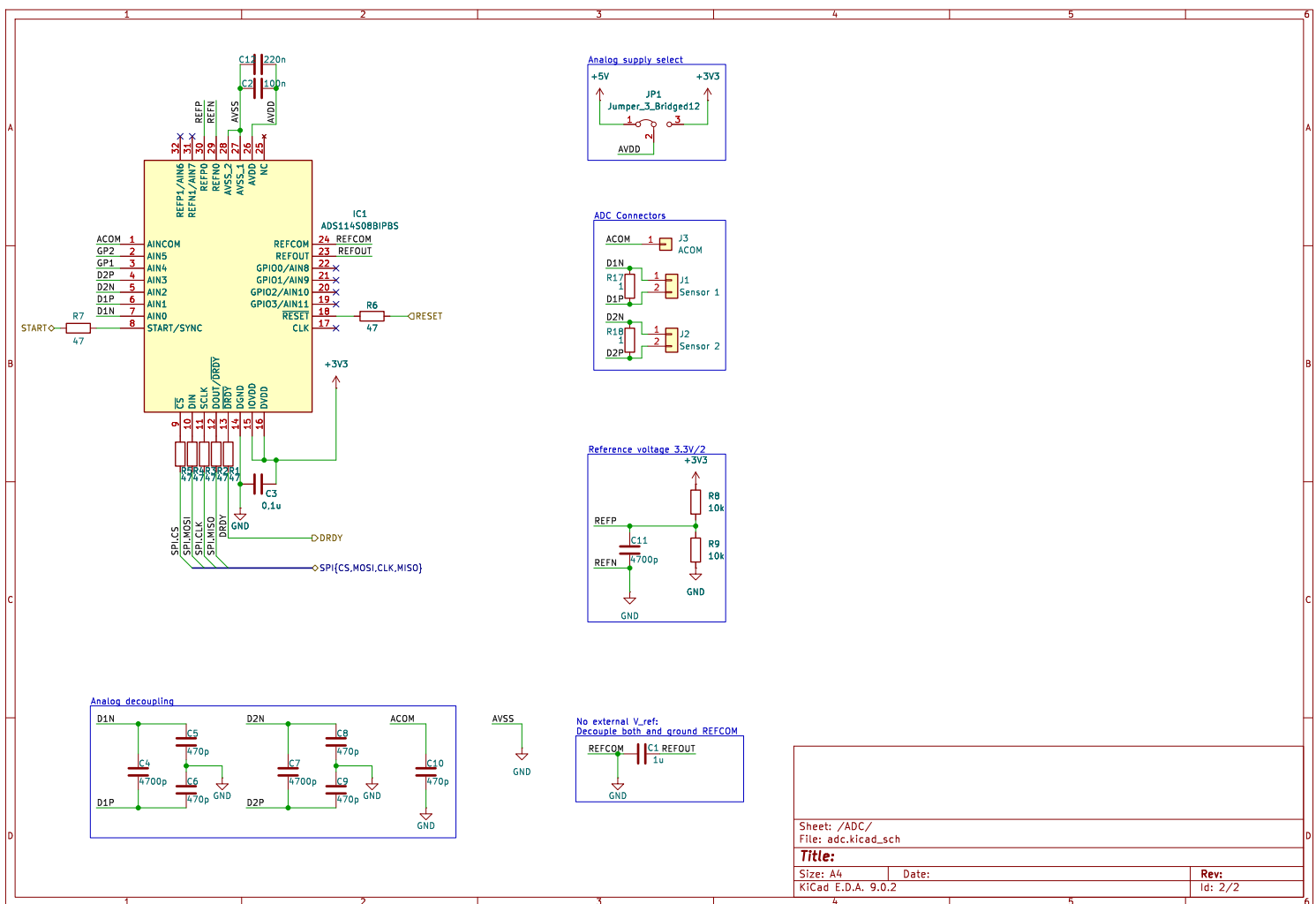
---

---

## C. Hardware Implementation

---





---

---

## **D. Risk Assessment NOVA**

---

# Fachgebiet Resilient Cyber-Physical Systems - Risk Assessment

Activity being assessed	Use of Voltera NOVA printer								
Location	RP B013								
Reference	200001								
Assessment date	14. Jan 25								
Review date									
Description of activity	Operation of Voltera NOVA printer located in RP B013 (S2 02 B013)								
Hazards	What harm might occur, and to whom?	Existing control measures	Risk rating	Additional control measures	Residual risk				
Contact with moving parts	Personal injury to user:- trapping and crushing	Keep hands outside of the printer enclosure whilst it is in operation.	L 1 S 2 RR 2						
Contact with smart dispenser and precision nozzle	Personal injury to user:- cuts and burns	Be careful when handling precision nozzles and the complete smart dispenser. Make sure hands are clear when the smart dispenser is in use and the system is moving.	L 1 S 2 RR 2						
Contact with electrical pins of the Module Hub	Personal injury to user:- electrical shocks	Never touch the electrical pins on the module hub when the locking lever is engaged.	L 1 S 2 RR 2						
Danger of shrapnel on breaking of Smart Probe	Personal injury to user and others in area whilst printer is operating:- Damage to eyes up to vision loss	Wear eye protection, especially when using custom fixturing, printing 3D structures, or when mounting accessories.	L 1 S 2 RR 2						
Exposure to chemicals and nano particles during ink handling	Personal injury to user and others in area whilst printer is operating:- respiratory damage and chemical hazards.	Only use approved, commercially available materials. Read the safety datasheet (SDS) of every ink prior to operation. Perform appropriate measures to mitigate risks stated in the SDS. Wear protective gloves when needed	L 1 S 3 RR 3						
Long exposure to loud noise	Personal injury to user and others in area whilst printer is operating:- Damage to ears or hearing ability	When NOVA pumps run above 30% duty cycle for extended periods of time, wear hearing protection	L 3 S 1 RR 3						

Lifting of heavy equipment

Personal injury to user carrying NOVA weighs 35 kg (77 lbs) and should always be the device:- Muscle strain or back injury

lifted by two people to avoid injury. Use proper lifting technique when relocating. Place NOVA carefully, as dropping the equipment can cause serious harm. When moving NOVA, each person should lift by the base with two hands.

All users of the machine must read the manual carefully before using NOVA.

<https://docs.voltera.io/nova/downloads/nova-user-manual>

Operating NOVA requires knowledge of the safety/ datasheet contents of every ink used in the process.

Safety datasheets for inks supplied by Voltera can be found at:

<https://docs.voltera.io/nova/downloads/safety-data-sheets>

2

1

2

2

1

2

Assessment created by  
Persons consulted

Philipp Macher  
Roderich Groß



## **E. SC1502**

---

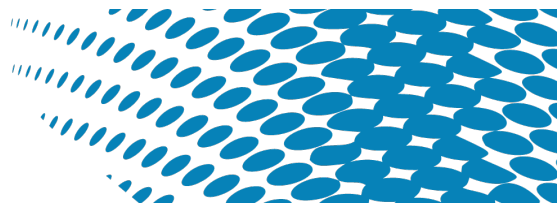
---

### **E.1. Data Sheet**

---

# SC1502

## Stretchable Printed Carbon Conductor



### Product Description

ACI SC1502 is a carbon-filled conductor for printed circuitry and devices on elastomeric substrates. It can be dried at low temperatures to accommodate sensitive substrates and devices. After curing, the ink has good conductivity and offers excellent elongation and flexibility. SC1502 has been formulated for superior adhesion to thermoplastic urethanes (TPU). It is compatible with ACI's other stretchable materials and can be printed over the silver grades in sensor applications to limit silver migration.

### Product Benefits

- Superior stretch performance on TPU offering elongation greater than 200%
- Excellent resistivity and rapid return after strain
- Excellent adhesion to TPU
- Low cure temperature (80°C) is possible for temperature sensitive materials
- Compatible with other products in ACI's stretchable electronics platform

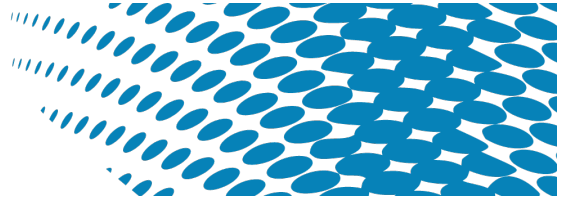
Typical Performance	
Volume resistivity 135°C for 15 min in box oven	< 236 Ω/square/mil < 0.6 Ω·cm
Maximum Elongation <sup>1</sup>	>200%
Adhesion <sup>2</sup>	5B
<sup>1</sup> 2 mm wide trace cured on TPU substrate <sup>2</sup> Method based on ASTM D3359 Method B	
Typical Properties as Supplied	
Physical State	Viscous black paste
Viscosity <sup>3</sup>	60 Pa·s
Density	1.08 g/cm <sup>3</sup>
Percent Solids <sup>4</sup>	25%
Shelf Life at 20°C	6 Months
Processing	
Deposition methods	Screen printing; micro dispense
Curing Time and Temperatures	15 min in box oven ≥ 120°C < 5 min in industrial conveyor oven at ≥120°C
Recommended Screen Meshes	200/230 Stainless Steel
Recommended Squeegee	RKS Carbon BW or S HQ
Coverage for Recommended meshes	43/33 m <sup>2</sup> /kg
Recommended Cured Thickness <sup>5</sup>	6-12 μm
Mixing	Slow thorough mix, avoid inducing bubbles, fixed spatula in rotating jar ideal <sup>6</sup>
Recommended Thinner/Diluent	TD8106
Clean Up Solvents	Acetone/MEK/Similar Solvents

<sup>3</sup> Measured on Anton Paar MCR302 Rheometer at 10<sup>-1</sup> sec shear rate at 25°C

<sup>4</sup> 150°C for 120 min in box oven

<sup>5</sup> Double print wet on wet or dry can be used to increase deposition thickness

<sup>6</sup> AT-LM4 Stirring Type Mixer (E211) recommended



## Contact ACI

Email: [info@acimaterials.com](mailto:info@acimaterials.com)  
Phone: (805) 324-4486  
Website: [www.acimaterials.com](http://www.acimaterials.com)

## Mailing and Shipment Address

ACI Materials, Inc.  
44 Castilian Drive  
Goleta, CA 93117

## Caution

Proper industrial safety precautions should be exercised in using these products. Use with adequate ventilation. Avoid prolonged contact with skin or inhalation of any vapors emitted during use or heating of these compositions. The use of safety eye goggles, gloves or hand protection creams is recommended. Wash hands or skin thoroughly with soap and water after using these products. Do not eat or smoke in areas where these materials are used. Refer to appropriate SDS information.

## Disclaimer

The product information and recommendations contained herein are based on data obtained by tests we believe to be accurate, but the accuracy and completeness thereof is not guaranteed. No warranty is expressed or implied regarding the accuracy of these data, the results obtained from the use hereof, or that any such use will not infringe any patent. ACI Materials, Inc. assumes no liability for any injury, loss, or damage, direct or consequential, arising out of its use by others. This information is furnished upon the condition that the person receiving it shall make their own tests to determine the suitability thereof for their particular use, before using it. User assumes all risk and liability whatsoever in connection with their intended use. ACI Materials' only obligation shall be to replace such quantity of the product proved defective.

---

---

## **E.2. Safety Data Sheet**

---



SC1502  
SDS Version 4.0

[www.acimaterials.com](http://www.acimaterials.com)

## SAFETY DATA SHEET

### Section 1: Identification of the substance / mixture and of the company / undertaking

**Product Identifier:** SC1502

**Other Means of Identification:** Stretchable Carbon Conductor

**Recommended use of the chemical and restrictions on use:** None identified

**Supplier:**

ACI Materials, Inc.  
44 Castilian Drive  
Goleta, CA 93117  
1 (805) 324-4486

**Emergency Phone Number:**

For emergency health, safety and environmental information, call 1 (805) 570-1071.

### Section 2: Hazards Identification

**Classification of the substance or mixture:**

Eye irritation	Category 2
Suspected carcinogen	



**Symbols:**

**Signal word:** Warning

**Hazard Statements:**

H319 Causes serious eye irritation.  
H351 Suspected of causing cancer.

**Precautionary Statements:**

P264 Wash skin thoroughly after handling.  
P280 Wear protective gloves/ protective clothing/ eye protection/ face protection.  
P305 + P351 + P338: IF IN EYES: Rinse cautiously with water for several minutes. Remove contact lenses, if present and easy to do. Continue rinsing.  
P337 + P313: If eye irritation persists: Get medical advice/ attention.

**Describe any hazards not otherwise classified:** No additional information.

**Section 3: Composition / Information on ingredients**

Chemical Name	CAS Number	Concentration, %
Carbon Black	1333-86-4	1 – 10
Component "A"	Proprietary	25 – 40

Remaining components are non-hazardous or present in amounts below reportable limits.

Exact percentage values for components are proprietary in accordance with 29 CFR 1910.1200(i).

**Section 4: First-aid measures**

**Description of First aid measures**

**General:** If irritation or other symptoms occur or persist from any route of exposure, remove the affected individual from the area: see a physician / get medical attention.

**Inhalation:** Move person to fresh air. If not breathing, give artificial respiration. Consult a physician.

**Skin contact:** Immediately remove contaminated clothing and shoes. Wash the affected area with plenty of soap and water. If skin irritation occurs: Get medical advice / attention.

**Eye contact:** Rinse immediately with plenty of water also under the eyelids for at least 15 minutes. Consult a physician.

**Ingestion:** Do not induce vomiting. Never give anything by mouth to an unconscious person. Rinse mouth with water. Consult a physician.

**Most important symptoms/effects, acute and delayed:** The most important known symptoms and effects are described in Section 2. See Section 11 for additional information.

**Indication of immediate medical attention and special treatment needed:** No data available.

#### **Section 5: Fire-fighting measures**

**Suitable extinguishing media:** Use water spray, alcohol-resistant foam, dry chemical or carbon dioxide.

**Unsuitable extinguishing media:** Do not use a solid water stream as it may scatter and spread fire.

**Specific hazards arising from the mixture:** Carbon oxides.

**Specific protective equipment and precautions for fire-fighters:** Use personal protective equipment. Wear self-contained breathing apparatus for firefighting if necessary.

#### **Section 6: Accidental release measures**

**Personal precautions, protective equipment, and emergency procedures:** Use personal protective equipment. Wear suitable protective clothing, gloves and eye / face protection. Avoid breathing vapors or gas. Ensure adequate ventilation. Evacuate personnel to safe areas. Eliminate ignition sources.

**Methods and materials for containment and cleaning up:** Approach suspected leak areas with caution. Contain spillage. Soak up with inert absorbent material and dispose of as hazardous waste. Place in appropriate chemical waste container. Do not let this chemical enter the environment.

#### **Section 7: Handling and storage**

**Precautions for safe handling:** Avoid contact with skin and eyes. Avoid inhalation of vapor. Keep away from sources of ignition. Use under well-ventilated conditions. Provide eyewash fountains and safety showers in the work area.

**Conditions for safe storage, including any incompatibilities:** Keep containers tightly closed in a dry, cool and well-ventilated place. Store this material away from incompatible substances (see section 10). Keep container closed when not in use.

#### Section 8: Exposure controls/personal protection

##### Control Parameters:

Component	CAS No.	Value	Control Parameter	Basis
Carbon Black, amorphous	1333-86-4	TWA (inhalable fraction)	3.5 mg / m <sup>3</sup>	EH40 WEL
Carbon Black, amorphous	1333-86-4	STEL (inhalable fraction)	7.0 mg / m <sup>3</sup>	EH40 WEL

**Appropriate engineering controls:** Handle in accordance with good industrial hygiene and safety practice. Wash hands before breaks and at the end of the workday.

##### Individual protection measures, such as personal protective equipment:

**Eye / face protection:** Safety glasses with side shields.

**Skin and body protection:** Wear chemical resistant (impervious) gloves. Wear clean, body-covering clothing.

**Respiratory Protection:** Where risk assessment shows air-purifying respirators are appropriate use a full-face respirator with multi-purpose combination respirator cartridges as a backup to engineering controls. If workplace exposures are exceeded respiratory protection should be used.

**Further Information:** Provide readily accessible eye wash stations and safety showers.

#### Section 9: Physical and chemical properties

**Appearance:** Black ink.

**Odor:** Mild

**Odor Threshold:** No data available

**pH:** No data available

**Melting point/freezing point:** No data available  
**Initial boiling point and boiling range:** 97 – 235 °C (Lowest boiling point of a component)  
**Flash point:** 109 °C (228 °F) (Lowest flash point of a component)  
**Evaporation rate:** No data available  
**Flammability (solid, gas):** No data available  
**Upper/lower flammability or explosive limits:** No data available  
**Vapor pressure:** No data available  
**Vapor density:** No data available  
**Relative density:** No data available  
**Solubility:** No data available  
**Partition coefficient: n-octanol/water:** No data available  
**Auto-ignition temperature:** No data available  
**Decomposition temperature:** No data available  
**Viscosity:** No data available.  
**Other Information:** Amounts listed are typical and do not represent a specification.

#### **Section 10: Stability and reactivity**

**Reactivity:** No data available.

**Chemical stability:** Stable under recommended storage conditions.

**Possibility of hazardous reactions:** No data available.

**Conditions to avoid:** Heat, flames and sparks.

**Incompatible materials:** Strong oxidizing agents, acids, bases, peroxides.

**Hazardous decomposition products:** Carbon oxides, isocyanates.

#### **Section 11: Toxicological information**

**Information on toxicological effects:**

**Information on the likely routes of exposure:** Product test data is not available. Toxicological information appears in this section when the constituent data is available.

**Numerical measures of toxicity:**

<u>Chemical Name</u>	<u>Oral LD50</u>	<u>Species</u>	<u>Dermal LD50</u>	<u>Species</u>
Component "A"	4,290 mg/kg	Rat	5,990 µL/kg	Rabbit

**Symptoms / effects, acute and chronic:** (Hexano-6-lactone): Irritating to eyes.

**Carcinogenicity.**

Carbon black is considered possibly carcinogenic to humans and classified as a IARC Group 2B carcinogen because there is sufficient evidence in experimental animals with inadequate evidence in human epidemiological studies.

**Section 12: Ecological Information**

**Ecotoxicity (aquatic and terrestrial, where available):** There is no data available for this product.

Ecotoxicological information appears in this section when such data is available for the components of the mixture.

<u>Chemical Name</u>	<u>LC50</u>	<u>Species</u>
Component "A"	280mg/L, 96h static	Poecilia reticulata

**Persistence and Degradability** (Hexano-6-lactone): Soluble in water. Persistence is unlikely based on information available.

**Section 13: Disposal Considerations**

Dispose of container and unused contents in accordance with federal, state and local requirements.

**Section 14: Transport Information**

**DOT – (US)**

Not dangerous goods

**IMDG**

Not dangerous goods

**IATA**

Not dangerous goods

## Section 15: Regulatory Information

Safety, health and environment regulations / legislation specific for the product:

### **U.S. federal and state regulations / legislation:**

This SDS has been prepared in accordance with the hazard criteria of the OSHA Hazard Communication Standard, 29 CFR 1910.1200.

### **SARA 302 Components**

No chemicals in this material are subject to the reporting requirements of SARA Title III, Section 302.

### **SARA 311/312 Health Hazards**

See Section 2 for more information.

### **SARA 313 Components**

No chemicals in this material are subject to the reporting requirements of SARA Title III, Section 313

### **United States TSCA Inventory**

All components of this product are in compliance with the inventory listing requirements of the U.S. Toxic Substances Control Act (TSCA) Chemical Substances Inventory.

### **California Proposition 65:**

This product contains a chemical known to the State of California to cause cancer, birth defects, or any other reproductive harm.  
Carbon black

## Section 16: Other Information

**Revision date:** June 6, 2023.

### **Nomenclature:**

LC = Lethal concentration

LD = Lethal dose

ND = No Data

STEL = Short Term Exposure Limit

TWA = Time weighted average

WEL = Workplace Exposure Limits

#### **Other Information**

Applied Cavitation, Inc. is a registered trademark. All rights reserved.

#### **Disclaimer Notice**

This product is a complex mixture of liquids and solids. This SDS was prepared based upon the SDS of the raw materials used in the mixture.

ACI Materials, Inc. (ACI) encourages each customer or recipient of this SDS to study it carefully and consult appropriate expertise, as necessary or appropriate, to become aware of and understand the data contained in this SDS and any hazards associated with the product. The information herein is provided in good faith and believed to be accurate as of the issue date shown above, but ACI makes no representation as to its comprehensiveness or accuracy. No warranty, express or implied, is given. Regulatory requirements are subject to change and may differ between various locations. It is the buyer's/user's responsibility to ensure that its activities comply with federal, state, provincial or local laws. The information presented here pertains only to the product as shipped. Since conditions for use of the product are not under the control of ACI, it is the buyer's/user's duty to determine the conditions necessary for the safe use of this product. Due to the proliferation of sources for information such as manufacturer-specific SDSs, ACI is not and cannot be responsible for SDSs obtained from any source other than ACI. If you have obtained an ACI SDS from a non-ACI source or if you are not sure that an ACI source is current, please contact ACI for the most recent version.